ESTIMATING NEUTRINO FLUX FROM LOW MASS STELLAR MODEL USING MACHINE LEARNING TECHNIQUE

IRFAN MUQRI BIN ABD RAHMAN

FACULTY OF SCIENCE
UNIVERSITI MALAYA
KUALA LUMPUR

2024

ESTIMATING NEUTRINO FLUX FROM LOW MASS STELLAR MODEL USING MACHINE LEARNING TECHNIQUE

IRFAN MUQRI BIN ABD RAHMAN

FINAL YEAR PROJECT REPORT SUBMITTED IN PARTIAL FULFILMENT OF THE REQUIREMENTS FOR THE DEGREE OF BACHELOR OF SCIENCE IN PHYSICS

DEPARTMENT OF PHYSICS
FACULTY OF SCIENCE
UNIVERSITI MALAYA
KUALA LUMPUR

2024

UNIVERSITI MALAYA

ORIGINAL LITERARY WORK DECLARATION

Name of Candidate: IRFAN MUQRI BIN ABD RAHMAN (021214-01-0451)

Matric No: U2103688

Name of Degree: BACHELOR OF SCIENCE IN PHYSICS

Title of Project Paper ("this Work"):

ESTIMATING NEUTRINO FLUX FROM LOW MASS STELLAR MODEL USING MACHINE LEARNING TECHNIQUE

Field of Study: Experimental Physics

I do solemnly and sincerely declare that:

(1) I am the sole author of this Work;
(2) This Work is original;
(3) Any use of any work in which copyright exists was done by way of fair dealing and for permitted purposes and any excerpt or extract from, or reference to or reproduction of any copyright work has been disclosed expressly and sufficiently and the title of the Work and its authorship have been acknowledged in this Work;
(4) I do not have any actual knowledge nor do I ought reasonably to know that the making of this work constitutes an infringement of any copyright work;
(5) I hereby assign all and every rights in the copyright to this Work to the University of Malaya ("UM"), who henceforth shall be owner of the copyright in this Work and that any reproduction or use in any form or by any means whatsoever is prohibited without the written consent of UM having been first had and obtained;
(6) I am fully aware that if in the course of making this Work I have infringed any copyright whether intentionally or otherwise, I may be subject to legal action or any other action as may be determined by UM.

Candidate's Signature Date: January 16, 2025

Subscribed and solemnly declared before,

Witness's Signature Date: January 16, 2025

Name:

Designation:

ESTIMATING NEUTRINO FLUX FROM LOW MASS STELLAR MODEL USING MACHINE LEARNING TECHNIQUE

ABSTRACT

Lorem ipsum dolor sit amet, consectetuer adipiscing elit. Etiam lobortis facilisis sem. Nullam nec mi et neque pharetra sollicitudin. Praesent imperdiet mi nec ante. Donec ullamcorper, felis non sodales commodo, lectus velit ultrices augue, a dignissim nibh lectus placerat pede. Vivamus nunc nunc, molestie ut, ultricies vel, semper in, velit. Ut porttitor. Praesent in sapien. Lorem ipsum dolor sit amet, consectetuer adipiscing elit. Duis fringilla tristique neque. Sed interdum libero ut metus. Pellentesque placerat. Nam rutrum augue a leo. Morbi sed elit sit amet ante lobortis sollicitudin. Praesent blandit blandit mauris. Praesent lectus tellus, aliquet aliquam, luctus a, egestas a, turpis. Mauris lacinia lorem sit amet ipsum. Nunc quis urna dictum turpis accumsan semper.

MENGANGGARKAN FLUKS NEUTRINO DARIPADA MODEL BINTANG JISIM RENDAH MENGGUNAKAN TEKNIK PEMBELAJARAN MESIN

ABSTRAK

Lorem ipsum dolor sit amet, consectetuer adipiscing elit. Etiam lobortis facilisis sem. Nullam nec mi et neque pharetra sollicitudin. Praesent imperdiet mi nec ante. Donec ullamcorper, felis non sodales commodo, lectus velit ultrices augue, a dignissim nibh lectus placerat pede. Vivamus nunc nunc, molestie ut, ultricies vel, semper in, velit. Ut porttitor. Praesent in sapien. Lorem ipsum dolor sit amet, consectetuer adipiscing elit. Duis fringilla tristique neque. Sed interdum libero ut metus. Pellentesque placerat. Nam rutrum augue a leo. Morbi sed elit sit amet ante lobortis sollicitudin. Praesent blandit blandit mauris. Praesent lectus tellus, aliquet aliquam, luctus a, egestas a, turpis. Mauris lacinia lorem sit amet ipsum. Nunc quis urna dictum turpis accumsan semper.

ACKNOWLEDGEMENTS

Lorem ipsum dolor sit amet, consectetuer adipiscing elit. Etiam lobortis facilisis sem. Nullam nec mi et neque pharetra sollicitudin. Praesent imperdiet mi nec ante. Donec ullamcorper, felis non sodales commodo, lectus velit ultrices augue, a dignissim nibh lectus placerat pede. Vivamus nunc nunc, molestie ut, ultricies vel, semper in, velit. Ut porttitor. Praesent in sapien. Lorem ipsum dolor sit amet, consectetuer adipiscing elit. Duis fringilla tristique neque. Sed interdum libero ut metus. Pellentesque placerat. Nam rutrum augue a leo. Morbi sed elit sit amet ante lobortis sollicitudin. Praesent blandit blandit mauris. Praesent lectus tellus, aliquet aliquam, luctus a, egestas a, turpis. Mauris lacinia lorem sit amet ipsum. Nunc quis urna dictum turpis accumsan semper.

TABLE OF CONTENTS

LIST OF FIGURES

LIST OF TABLES

LIST OF SYMBOLS AND ABBREVIATIONS

EA : Example Abbreviation

LIST OF APPENDICES

CHAPTER 1: INTRODUCTION

Neutrino is one of the elementary particles in the fermion group and were theoretically invented in 1930 by Pauli to preserve energy–momentum conservation. It is a neutral particle which only has a very small mass and is only affected by gravitation and weak interaction. Neutrinos are known to be the most abundant particles in the universe after photon with a density of approximately 330 cm^{-3} pan universe (Athar & Singh, 2020). All these neutrinos come from a lot of sources, they are produced inside the sun, the earth, the entire atmosphere, during the birth, collision, and death of stars and huge flux of neutrinos is emitted during supernovae explosions. In stars like our sun the amount of neutrinos produce is very abundant as it is part of the fission process through beta decay and electron capture, for example in the proton-proton chain reaction where 2 ^{1}H fuses into one ^{2}H converting one of the protons into neutron (Iliadis, 2007). And due to it having small collision cross-section most of these neutrinos go out of the sun without being blocked going out to every direction, a lot of them pass through us. Neutrino flux is the measure of the number of neutrinos flowing through, on earth we use detectors such as the Super Kamiokande.

Machine learning is a technique that improves system performance by learning from experience via computational means (Zhou, 2021). In physics, especially through recent decades, machine learning has taken its roots, especially in statistical analysis with a large amount of data. For example, it has been used in processing satellite data in atmospheric physics, in weather forecasts, predicting the behavior of systems of many particles, discovering functional materials and generating new organic molecules (Rodrigues, 2023).

We do have data for solar neutrinos from the sun which is a low mass stellar model from various of detectors from earth. However, for stars far away we must estimate the neutrino flux since there is no method to directly detect the neutrino. There are some theoretical calculations that can be done to estimate the neutrino flux but, in this research, we plan to use machine learning to do the estimation.

1.1 Problem Statement

Neutrinos are present in huge quantities owing to various astrophysical phenomena such as those in a stellar medium like the Sun. Although solar neutrino flux is able to be measured on the Earth by using a detector like Super Kamiokande, neutrinos emitted from distant stars and the physics of their detection still presents a problem because of the difficulty in interaction and the detection of such distant and sparse interactions by current technology. There is no proper means of detecting neutrino radiation from stellar sources at the present time, though theorists continue to make predictions based on elaborate computations.

To address these issues, machine learning approaches, which are particularly efficient when it comes to complex data processing tasks and prediction problems located in various physics, would be one of the available options. This study aims to solve the problem by estimating the neutrino flux from a low mass stellar model through the use of a machine learning approach. Here we will try to construct and train a supervised machine learning model aimed at predicting neutrino flux from stars which are not accessible by direct observation, utilizing available solar neutrino flux data and theoretical models.

1.2 Research Questions

The research aims to answer the following questions:

1. What is the neutrino flux production beyond the Standard Solar Model in low mass stars?
2. Is machine learning able to give the best estimate in the current solar neutrino productions?

1.3 Research Objectives

The research aims to achieve the following objectives:

1. To train using machine learning techniques to estimate neutrino flux that can mimic real flux measured
2. To test the accuracy of linear regression from the machine learning in estimating neutrino flux

1.4 Relevance of Research

1. Provide new understanding in the neutrino flux or production beyond Standard Solar Model
2. To test the robustness of the linear regression in handling the neutrino flux calculation from low mass stars grid.

CHAPTER 2: LITERATURE REVIEW

2.1 Stellar Model

A stellar model is a mathematical model that describes a star structure and evolution. Stellar structure models describe the internal structure of a star in detail and make predictions about the luminosity, the color and the future evolution of the star. Different classes and ages of stars have different internal structures, reflecting their elemental makeup and energy transport mechanisms. Stellar evolution is the process by which a star changes over the course of its lifetime (Bertulani, 2013). A stellar evolutionary model is a mathematical model that can be used to compute the evolutionary phases of a star from its formation until it becomes a remnant.

Example of a stellar model is the Standard Solar Model (SSM) which According to Fuller and Haxton (2022) trace the evolution of the Sun from its beginning i.e. when the collapse of the primordial gas cloud was halted by the turn-on of thermonuclear reactions, to today, 4.6 Gyears later, thereby predicting contemporary solar properties such as the composition, temperature, pressure, and sound-speed profiles and the neutrino fluxes. It's used to test the validity of stellar evolution theory. The SSM is used to test the validity of stellar evolution theory. In fact, the only way to determine the two free parameters of the stellar evolution model, the helium abundance and the mixing length parameter (used to model convection in the Sun), are to adjust the SSM to fit the observed Sun.

Stellar modelling is often done using computational software such as "Modules for Experiments in Stellar Astrophysics" (MESA) which is a suite of open source, robust, efficient, thread-safe libraries for a wide range. It is one-dimensional stellar evolution module, MESAstar, combines many of the numerical and physics modules for simulations of multiple different scenarios in stellar evolution ranging from very low mass to massive stars, including advanced evolutionary phases(Paxton et al., 2010). The net module implements nuclear reaction networks and is derived from publicly available code. It includes a "basic" network of eight isotopes: ^{1}H, ^{3}He, ^{4}He, ^{12}C, ^{14}N, ^{16}O, ^{20}Ne, and ^{24}Mg, and extended networks for more detailed calculations including coverage of hot CNO reactions, α-capture chains. This reaction rates can then be used to calculate data for the neutrinos.

2.2 Neutrino

An elementary particle first proposed by Pauli in 1931 and named by Fermi; the neutrino was to account for the missing energy released in β decay. Due to conservation of electric charge, it must be neutral, and conservation of angular momentum requires it to have a spin of $\frac{1}{2}$. There are two types of neutrinos emitted in β decay neutrino, e and antineutrino, e and they are emitted in β+ and β- decays respectively. The neutrino has a very small

cross section, σ of 1.2×10^{-43} cm^2 (Krane, 1991). Due to this, neutrinos can escape from the sun in about 2 seconds which is very fast compared to the 100,000 years for a photon (Rosso et al., 2018). The first neutrino was detected experimentally in the 1950s by Reines and Cowan using a nuclear reactor as the source where β- decays occur producing e.

2.3 Neutrino Sources

There are multiple sources of neutrino both on earth and extraterrestrial, for example the Cosmic Neutrino Background (CNB), Supernovae, Solar and Thermal neutrinos from the sun, Geoneutrinos and many more as shown in Figure 2.1 (Athar & Singh, 2020).

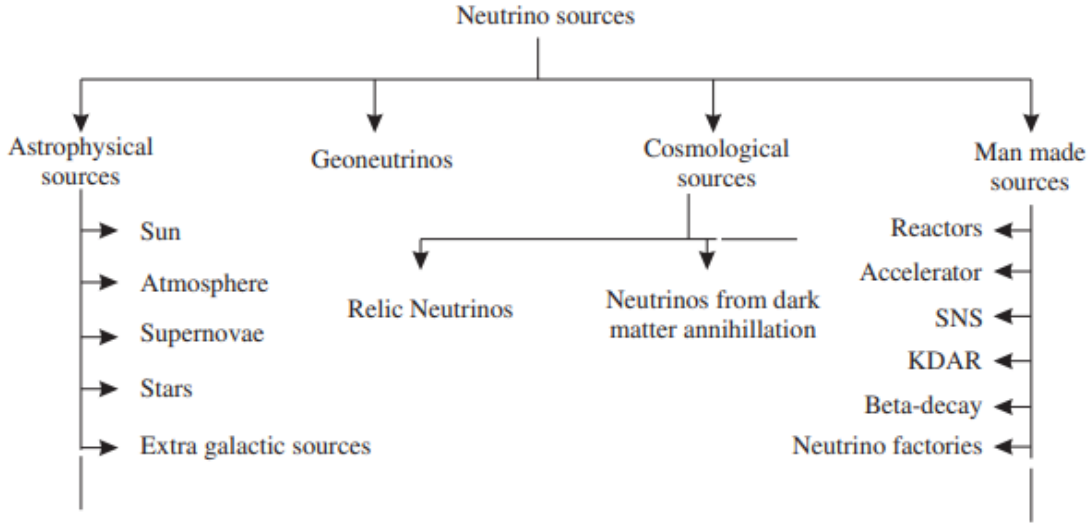

Figure 17.1 Different sources of neutrinos.

Figure 2.1: Neutrino sources.

Most of them produce neutrinos through β decays and electron(positron) capture like shown in Table 2.1 (Rosso et al., 2018):

Table 2.1: Most common reaction that produce ν.

Name	Reaction
β^- decays	$n \rightarrow p + e^- + \bar{\nu}_e$
β^+ decays	$p \rightarrow n + e^+ + \nu_e$
e^- capture	$e^- + p \rightarrow n + \nu_e$
e^+ capture	$e^+ + n \rightarrow p + \bar{\nu}_e$

that produce ν.

And unlike most other particles which are charged neutrinos can be assumed to come directly from their source as they are not deflected by magnetic field and unlike photons, neutrinos weakly interact making them able to pass through matter easily, the interaction length of a 1-TeV neutrino is about 2.5 million kilometers of water, or 250 kt cm^{-2}, whereas high-energy photons are blocked by a few hundred g cm^{-2} (Barenboim & Quigg, 2003).

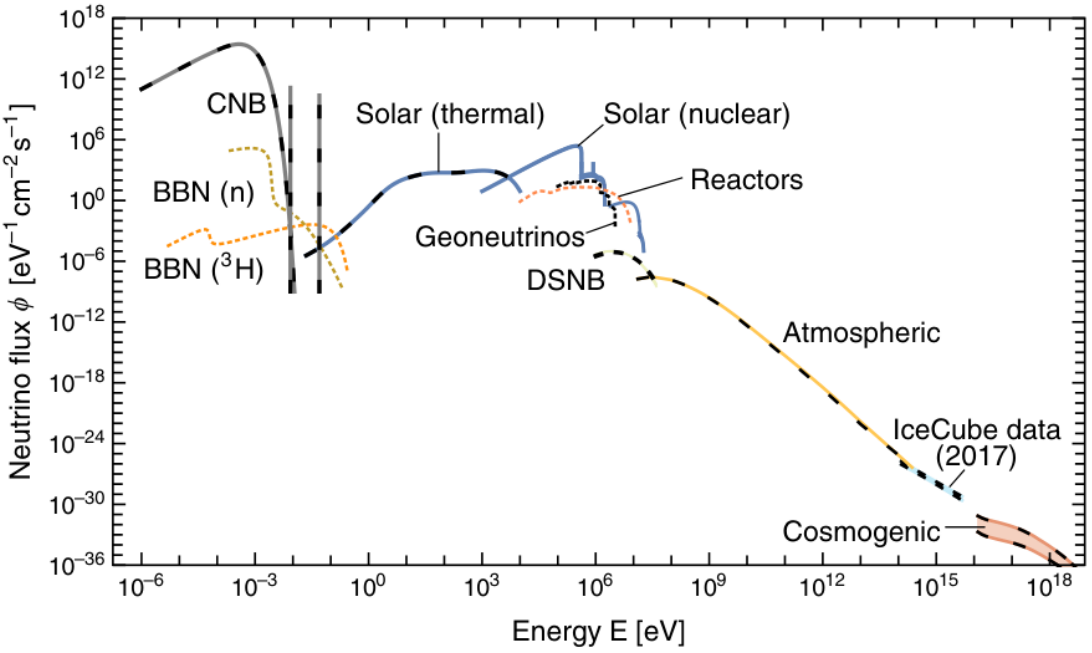

Figure 2.2: Grand Unified Neutrino Spectrum.

Figure 2.2 (Vitagliano et al., 2020) shows the fluxes from different neutrino sources. The range of energy for different sources is quite huge, spanning over 24 orders of magnitude.

2.4 Solar Neutrino

The sun through the thermonuclear fusion reaction produces a huge amount of e with energy the order of 1MeV. Since neutrino interaction with matter is weak, almost all the neutrino produced in the core goes out from the sun. The earth receives about 6×10^{10} cm^{-2} s flux of solar neutrinos. For the sun 2.3% of its nuclear energy production is in the form of MeV range electron neutrinos (Giunti & Kim, 2007). This comes from the effective nuclear reaction

$$4p + 2e \rightarrow 2^4He + 2\nu_e + 26.73MeV \tag{2.1}$$

Which comes from several reaction chains and cycles (Vitagliano et al., 2020).

Table 2.2: Reaction that produce neutrino in in the sun.

Channel	Flux	Reaction
pp chains (β^+)	Φ_{pp}	$p + p \rightarrow d + e^+ + \nu_e$
	$\Phi_{\rm B}$	$^8{\rm B} \rightarrow {}^8{\rm Be}^* + e^+ + \nu_e$
	$\Phi_{\rm hep}$	$^3{\rm He} + p \rightarrow {}^4{\rm He} + e^+ + \nu$
pp chains (EC)	$\Phi_{\rm Be}$	$e^- + {}^7{\rm Be} \rightarrow {}^7{\rm Li} + \nu_e$
		$e^- + {}^7{\rm Be} \rightarrow {}^7{\rm Li}^* + \nu_e$
	$\Phi_{\rm pep}$	$p + e^- + p \rightarrow d + \nu_e$
CNO cycle (β^+)	$\Phi_{\rm N}$	$^{13}{\rm N} \rightarrow {}^{13}{\rm C} + e^+ + \nu_e$
	$\Phi_{\rm O}$	$^{15}{\rm O} \rightarrow {}^{15}{\rm N} + e^+ + \nu_e$
	$\Phi_{\rm F}$	$^{17}{\rm F} \rightarrow {}^{17}{\rm O} + e^+ + \nu_e$
CNO Cycle (EC)	$\Phi_{\rm eN}$	$^{13}{\rm N} + e^- \rightarrow {}^{13}{\rm C} + \nu_e$
	$\Phi_{\rm eO}$	$^{15}{\rm O} + e^- \rightarrow {}^{15}{\rm N} + \nu_e$
	$\Phi_{\rm eF}$	$^{17}{\rm F} + e^- \rightarrow {}^{17}{\rm O} + \nu_e$

Table 2.3: Expected neutrino fluxes.

Branch	Flux, $10^6/({\rm cm}^2\ {\rm s})$	$E_\nu^{\rm max}$, MeV
pp	$59,800(1 \pm 0.006)$	0.420
^{7}Be	$4,930(1 \pm 0.06)$	0.862
pep	$144(1 \pm 0.01)$	1.442
^{8}B	$5.46(1 \pm 0.12)$	15.1
hep	$0.008(1 \pm 0.30)$	18.773
^{13}N	$278(1 \pm 0.15)$	1.199
^{15}O	$205(1 \pm 0.17)$	1.732
^{17}F	$5.28(1 \pm 0.20)$	1.740

Table2.2 (Vitagliano et al., 2020) shows the different reactions that produce neutrinos that can be detected on earth that the sun produces in its thermonuclear process. While table2.3 (Rosso et al., 2018) shows the expectation of the solar neutrino flux from each branch coming to earth. Referring to table Graph 1, we can see the shape of the flux in a solid blue line labelled "Solar (nuclear)".

2.5 Theoretical vs Experimental

2.5.1 Theoretical

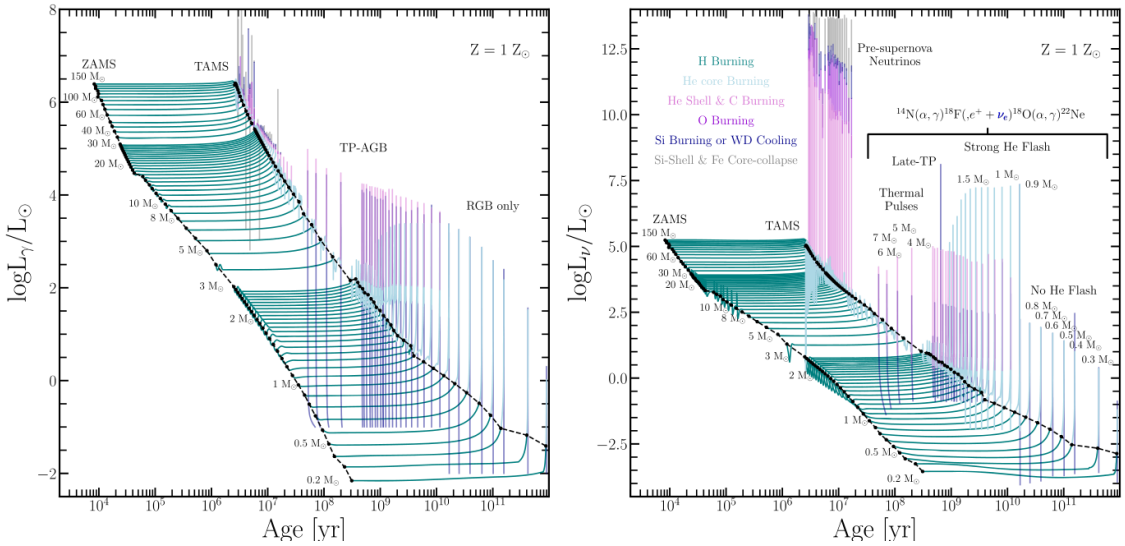

Figure 2.3: Light curve for photons(left) and neutrinos(right).

For the theoretical side of stellar physics, most of them are done in doing stellar modelling to predict structures and evolution of certain mass stars. Example of theoretical

work done in neutrino is Stellar Neutrino Emission across the Mass–Metallicity Plane done by (Farag et al., 2023b) where they explore neutrino emission from nonrotating, single-star models across six initial metallicities and 70 initial masses from the zero-age main sequence to the final fate shown in Graph 2.3. The data produced in the model are used in this research in order to train the model.

Since the time and computational power needed to run even one model is quite arduous, by using machine learning, the gap between the modelled grid can be predicted using machine learning.

2.5.2 Experimental

Due to neutrinos having an almost negligible mass and interact weakly with matter, the experiments that are required to detect them are usually done on a large scale in the range of km3 which can be setback by technological challenges (Addazi et al., 2022). Notable experiments include Super Kamiokande in Japan, the Sudbury Neutrino Observatory (SNO) in Canada, and the Jiangmen Underground Neutrino Observatory (JUNO) in China. Data from these experiments can validate the prediction obtained from a machine learning model.

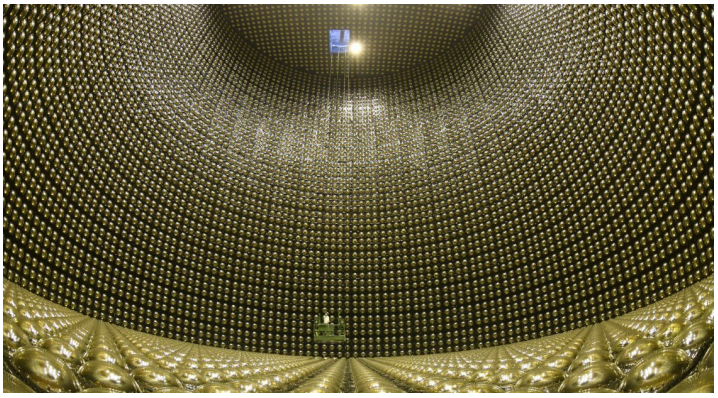

Figure 2.4: A stainless-steel tank, 39.3m diameter and 41.4m tall, filled with 50,000 tons of water. About 13,000 photo-multipliers are installed on the tank wall (*Overview — Super-Kamiokande Official Webiste*, n.d.).

2.6 Current Works

Dense neural network was proposed by Kopp et al. (2024) to estimate kinematic variable that cannot be observed directly in a neutrino interaction final state. The network was trained on simulated data and the DNN manage to predict the true neutrino energy based on observable components of the interactions.

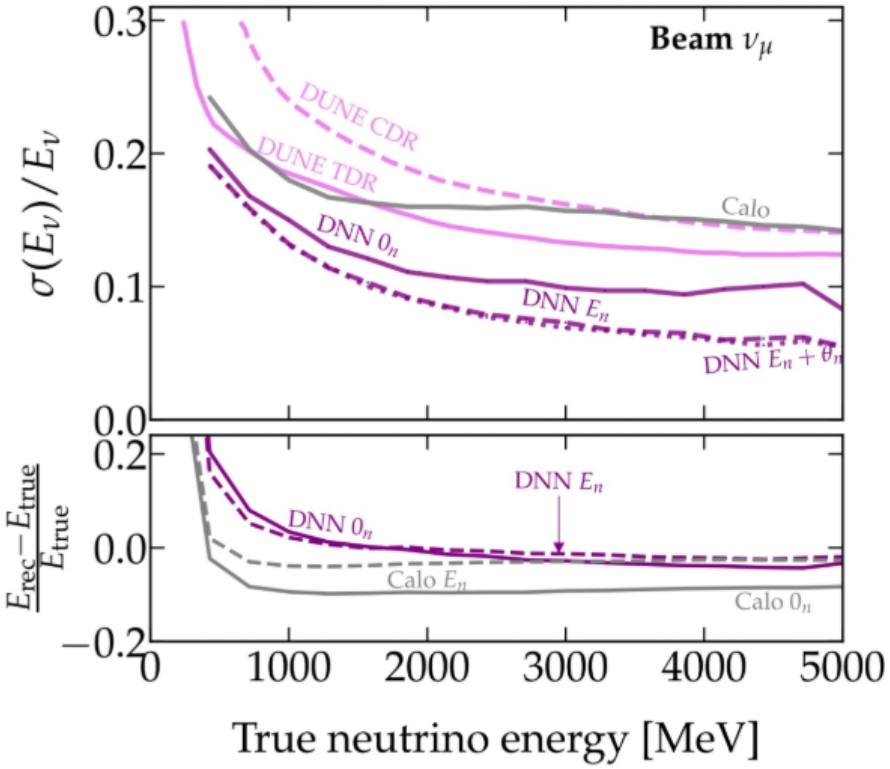

Figure 2.5: Top: Fractional neutrino energy resolution $\sigma(E_\nu)/E_\nu$. Bottom: Reconstruction bias for the DNN and the calorimetric method.

In the top of Graph 2.5 it shows fractional neutrino energy resolution $\sigma(E_\nu)/E_\nu$ as a function of neutrino energy with DNN based analyses with no information on final-state neutrons in solid purple, with limited information on the neutron energy in dashed purple, and with information on the neutron energy and direction in dotted purple. For comparison, they also include the energy resolutions anticipated in the DUNE CDR and TDR simulations in magenta, and the resolution of a simple calorimetric method assuming invisible neutrons in gray. In the bottom part we can see the reconstruction bias for the DNN compared to the calorimetric method. DNNs significantly outperform conventional approaches for energy reconstruction. When information on the energy of final-state neutrons is given, the improvement at high energies is a factor of two.

2.7 Machine Learning

Machine learning has been on the rise rapidly and can potentially revolutionize how we do sciences, including physics. According to Rodrigues (2023) even though machine learning can help solve fundamental problems in physics, many physicists still do not recognise the importance of these techniques. In physics, machine learning is often used in settings with complex problems and lots of data like in the large hadron collider (LHC) experiments where the data can reach up to ten of thousands of petabytes per year.

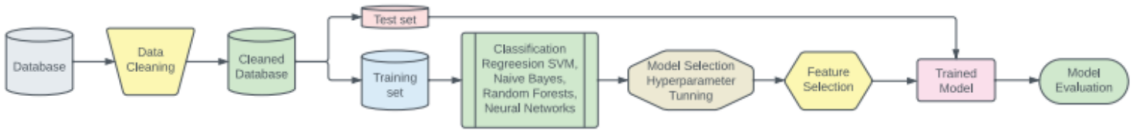

Figure 2.6: Supervise learning pipeline.

In Figure 2.6 (Rodrigues, 2023), usually in supervised learning 80% of data is used to train the model while 20% is for testing the model. In research done by (Niu et al., 2019), by using Bayesian neural network (BNN) which is a machine learning technique, they manage to get results that well reproduce the experimental data with very high accuracy and provide reasonable uncertainty in half-life prediction as shown in Figure 2.7 compared to prediction done using calculation.

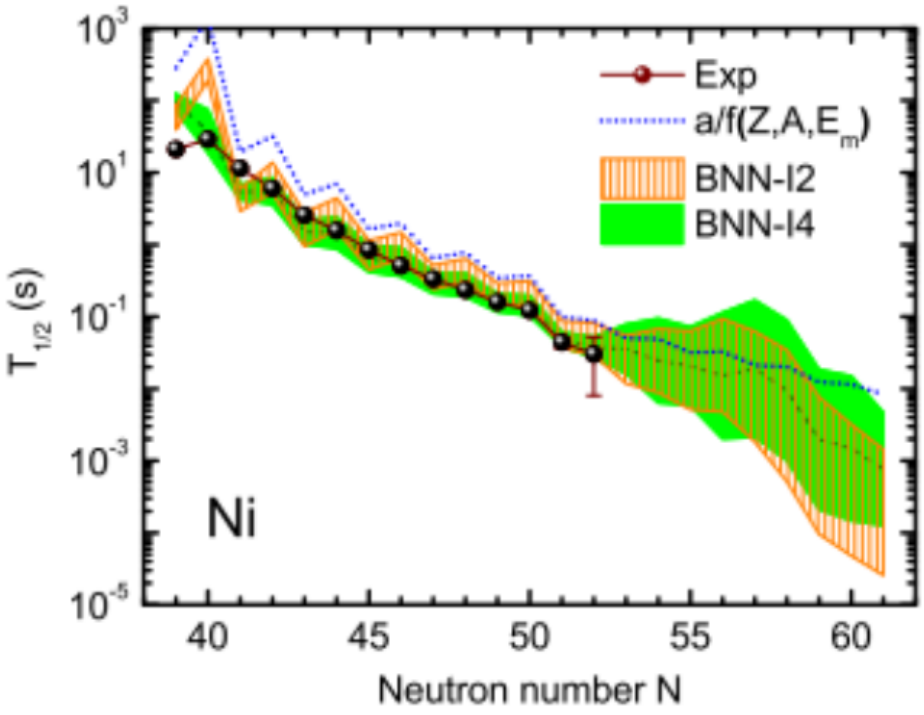

Figure 2.7: β decay half-life of Ni isotopes.

Where the experimental values in NUBASE2016 are denoted by spheres. The half-life predictions with calculation are shown by the dotted line, and their counterparts improved by BNN-I2 and BNN-I4 approaches, and their uncertainties are shown by vertical line hatched region and green hatched region, respectively. The mean predicted half-lives of

BNN-I4 approach are marked by the dashed line.

2.8 Linear Regression

Least squares is a regression analysis that does parameter estimation based on finding the minimum of the sum of the squares of the residuals. Linear least square can be used when there is a linear combination of parameters (Williams, 2016):

$$Y(x, \beta) = \sum_{j=1}^{m} \beta_j X_j \tag{2.2}$$

when letting the X and Y variables as matrices, the least square can be computed as follow:

$$L(D, \beta) = ||Y - X\beta||^2 = (Y - X\beta)^T (Y - X\beta) = Y^T Y - X^T Y\beta - X^T Y\beta + X^T X\beta^2 \tag{2.3}$$

where D is the set of all data. The gradient of the loss is then:

$$\frac{\delta L(D, \beta)}{\delta \beta} = \frac{\delta Y^T Y - X^T Y\beta - X^T Y\beta + X^T X\beta^2}{\delta \beta} = 2X^T Y + 2X^T X\beta \tag{2.4}$$

setting the gradient to zero then give us:

$$\hat{\beta} = (X^T X)^{-1} X^T Y \tag{2.5}$$

where $\hat{\beta}$ is the least square gradient.

CHAPTER 3: METHODOLOGY

3.1 Data

The data used was taken from (Farag et al., 2023a) which uses a mesa stellar evolution code that model the evolution from hydrogen burning all the way up to triple alpha burning stage.Data that was used in training the model are from 0.2 to 3 solar masses. The data is then separated into several section of linearity as shown below to minimise error: 0.2-0.4, 0.5-1.1, 1.2-1.4, 1.5-1.9, 2-2.3, 2.4-3.0

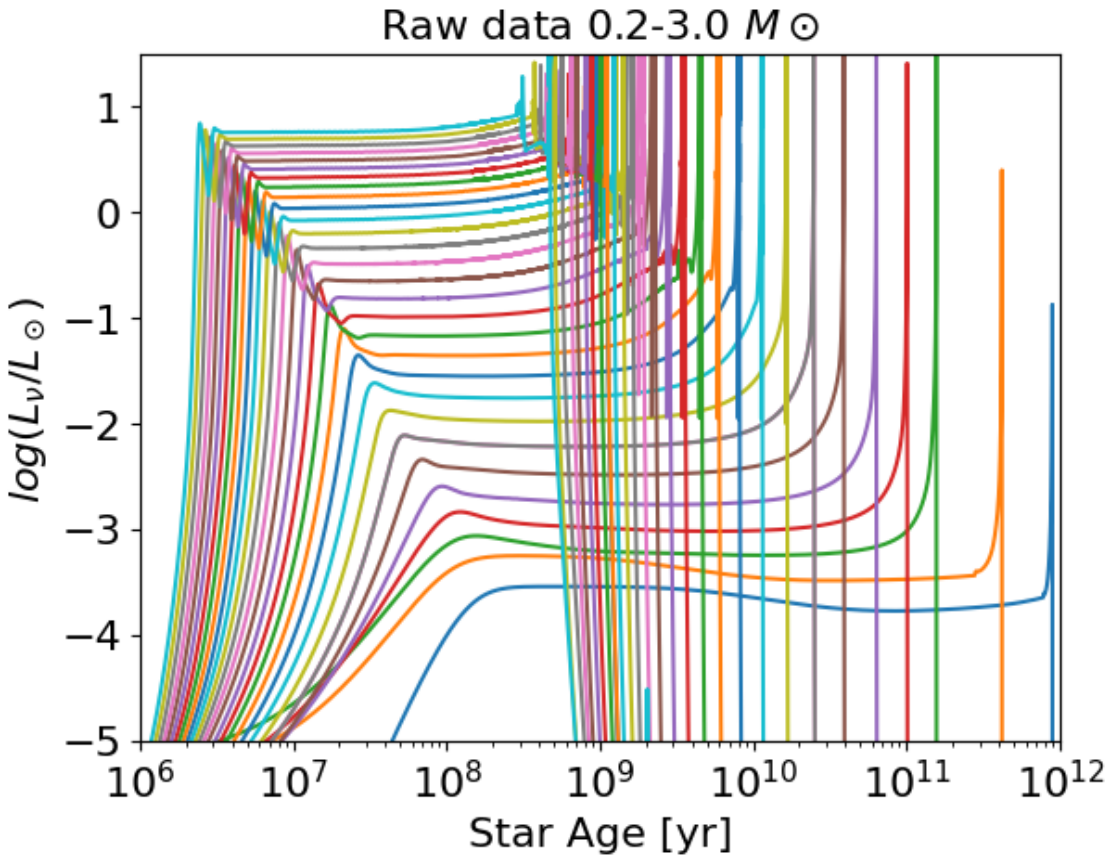

Figure 3.1: Raw data $0.2 - 3.0 M\odot$.

Figure 3.1 shows the raw data from the evolution code. The data was then cut to only include the hydrogen burning part for the linear regression.

3.2 Machine Learning

Sci Kit Learn was used, specifically the Linear Regression module:

$$y = \beta_0 + \beta_1 x_1 + \beta_2 x_2 + \beta_3 x_3 + \ldots + \beta_n x_n \tag{3.1}$$

where y is the independent variables, β_0 is the intercept, $\beta_1, \beta_2, \beta_3, \ldots, \beta_n$ is the coefficient.

The basis of linear regression is the same as $y = mx + c$ but sklearn used more coefficients to predict the model. Linear regression estimate coefficient such that the sum of error is very small 10^{-4} (the tolerance adopted by sklearn). This method is also known as the least square method.

In this project the code will calculate the gradient B (written as J) between the inputs which are the Masses and the Luminosity and the star ages.

$$\begin{bmatrix} m_1 \\ m_2 \\ m_3 \end{bmatrix} J = \begin{bmatrix} L_{11} & A_{11} & L_{12} & A_{12} & L_{13} & A_{13} \\ L_{21} & A_{21} & L_{22} & A_{22} & L_{23} & A_{23} \\ L_{31} & A_{31} & L_{32} & A_{32} & L_{33} & A_{33} \end{bmatrix} \tag{3.2}$$

where m is mass, L is luminosity and A is star age. Equation3.2 is the representation on how the data was arranged in order to do the linear regression method.

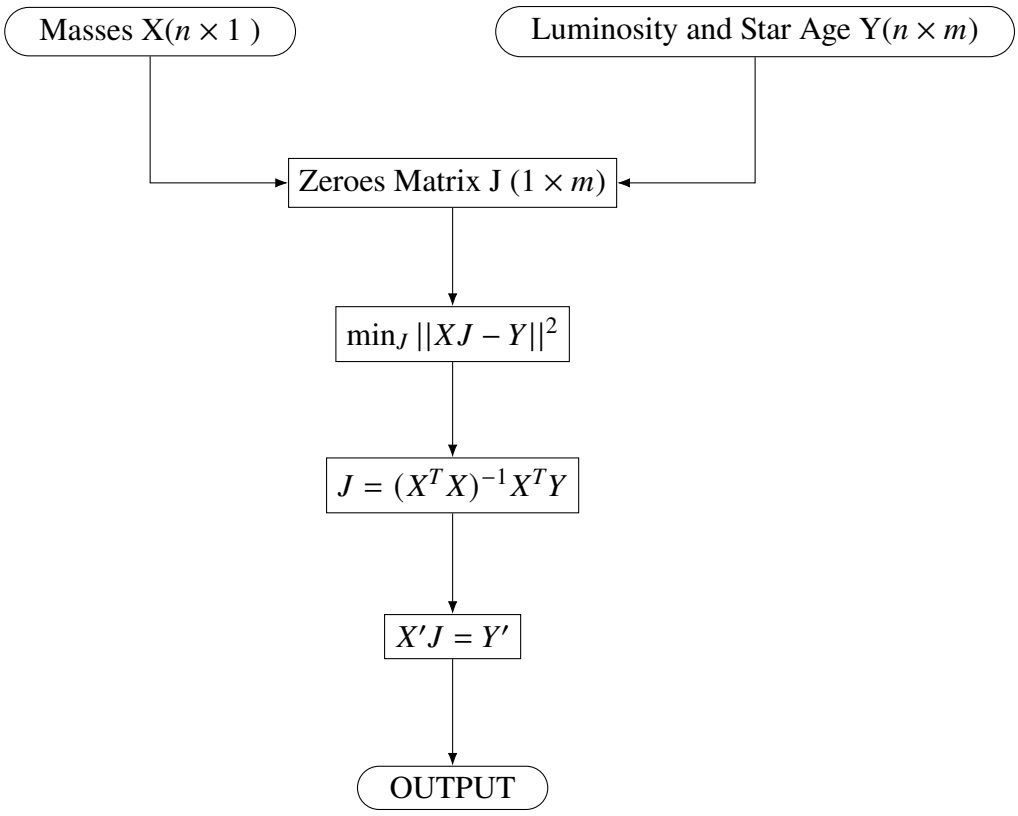

Figure 3.2: Flowchart of how the code does the linear regression.

Figure 3.2 shows the flow of how the code does the linear regression. The code will take input Masses in the form of X($n \times 1$) matrix and Luminosity and Star Age as Y($n \times m$) matrix. The code will then generate a zeros matrix J($1 \times m$). The J will then be calculated using Equation2.5 and then used in prediction.

$$e = \sqrt{(x_p - x_g)^2 + (y_p - y_g)^2} \tag{3.3}$$

Then using the Equation 3.3, the error was calculated in term of the offset between predicted and grid data per mass.

$$\text{Flux} = \frac{L}{4\pi r^2} \tag{3.4}$$

Using the prediction from the linear regression, we can then use the Formula 3.4 to calculate for flux of distant low mass star of known mass and distant from earth.

4.1 Single Model vs Multi Model

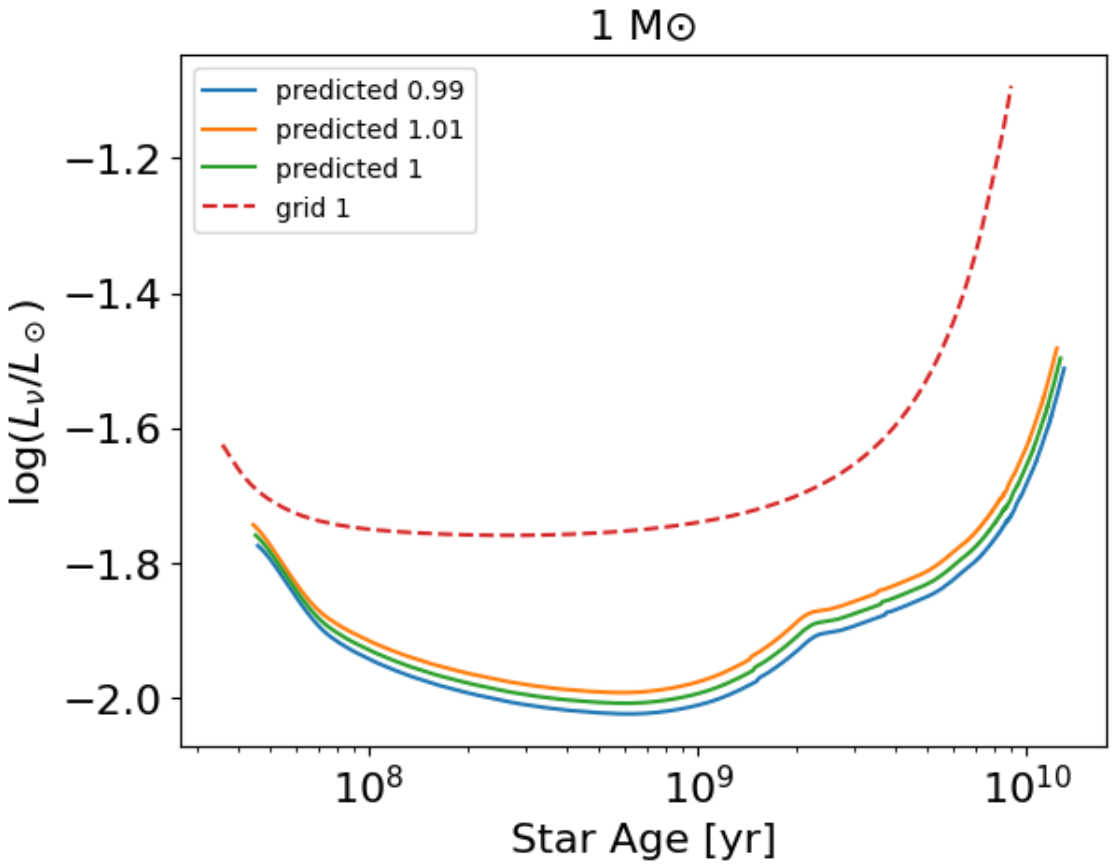

(a) Sun $1M\odot$ Single Testing Data.

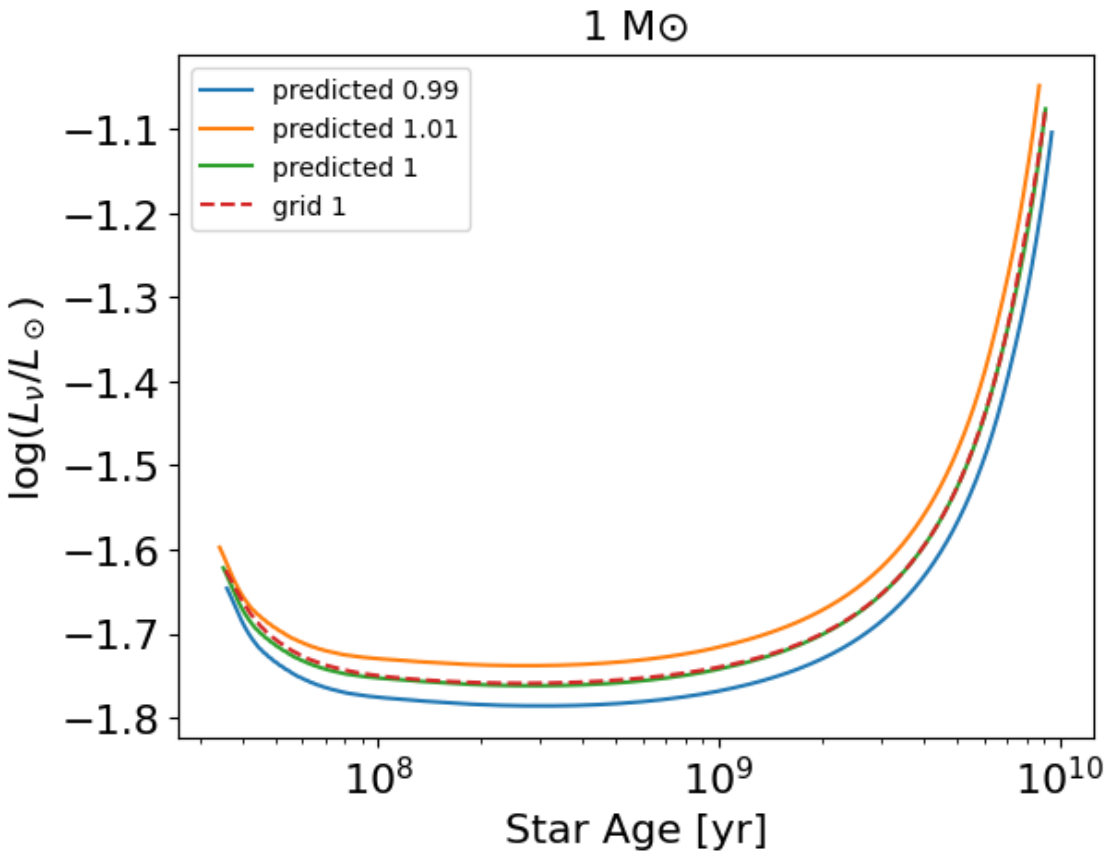

(b) Sun $1M\odot$ Multi Model($0.5 - 1.1M_{\odot}$) Testing Data.

Figure 4.1: Prediction Model testing grid $1M$

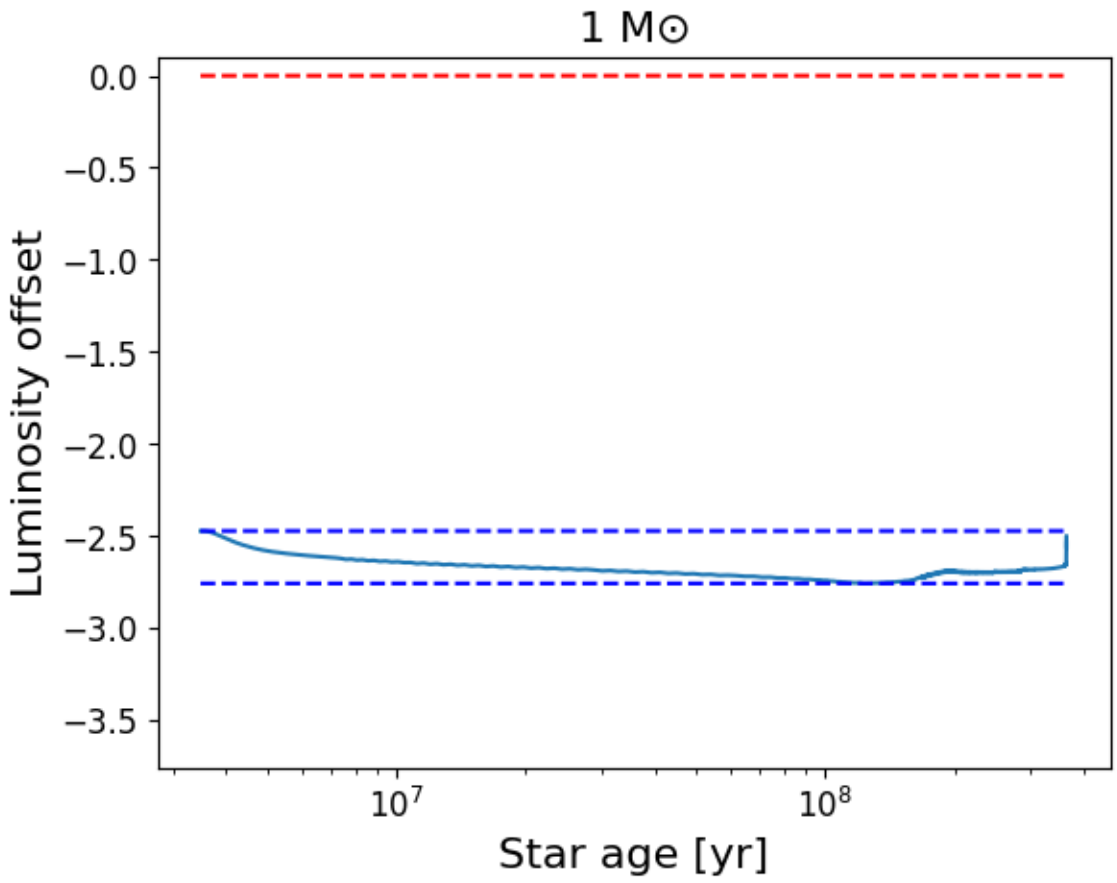

(a) Luminosity Offset for $1M\odot$.

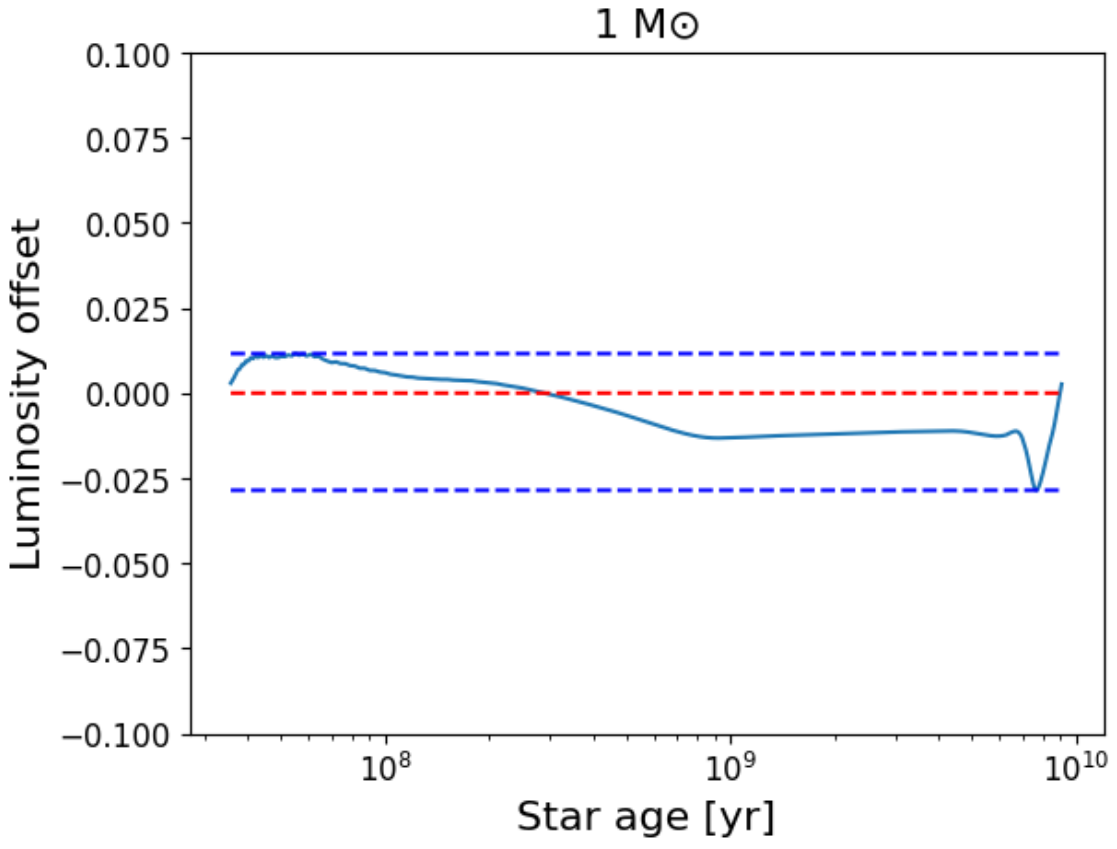

(b) Multimodel Error for $1M\odot$.

Figure 4.2: Comparison of Luminosity offset for Single Model and Multi Model($0.5 - 1.1M_\odot$) for $1M_\odot$

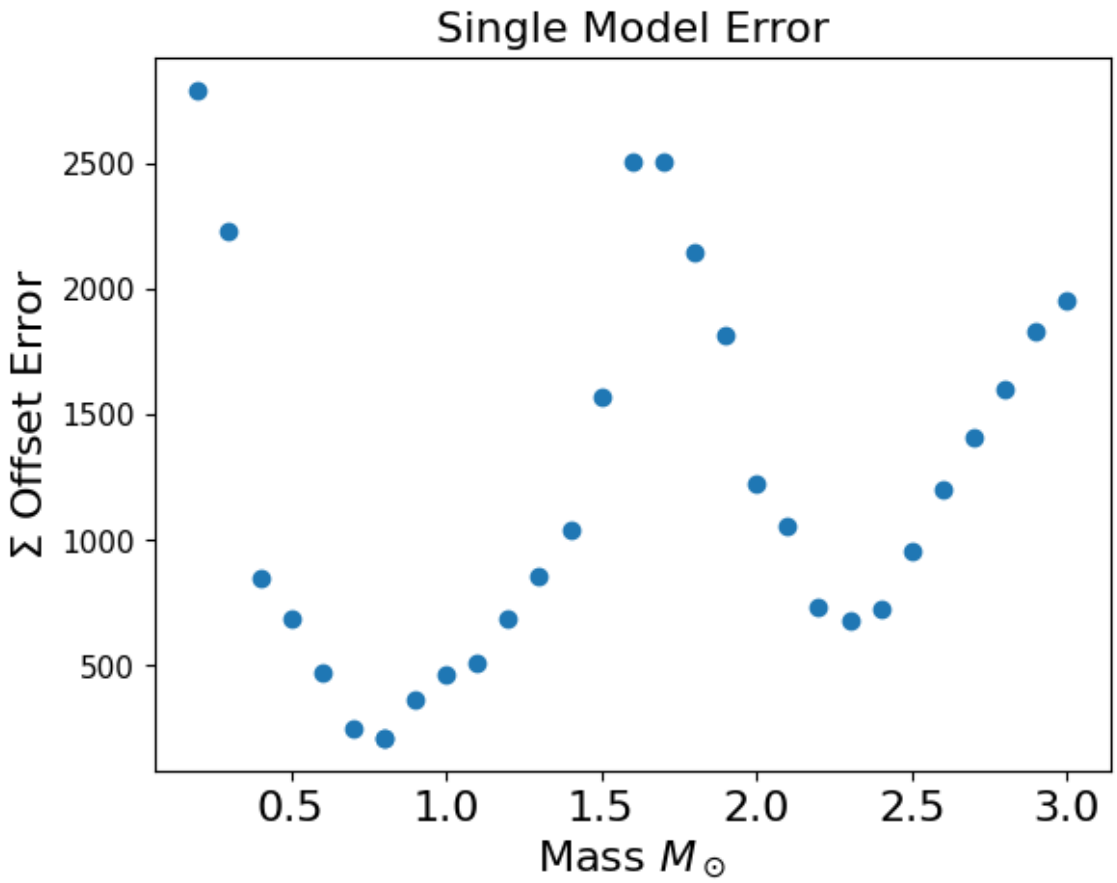

(a) Single Model Error.

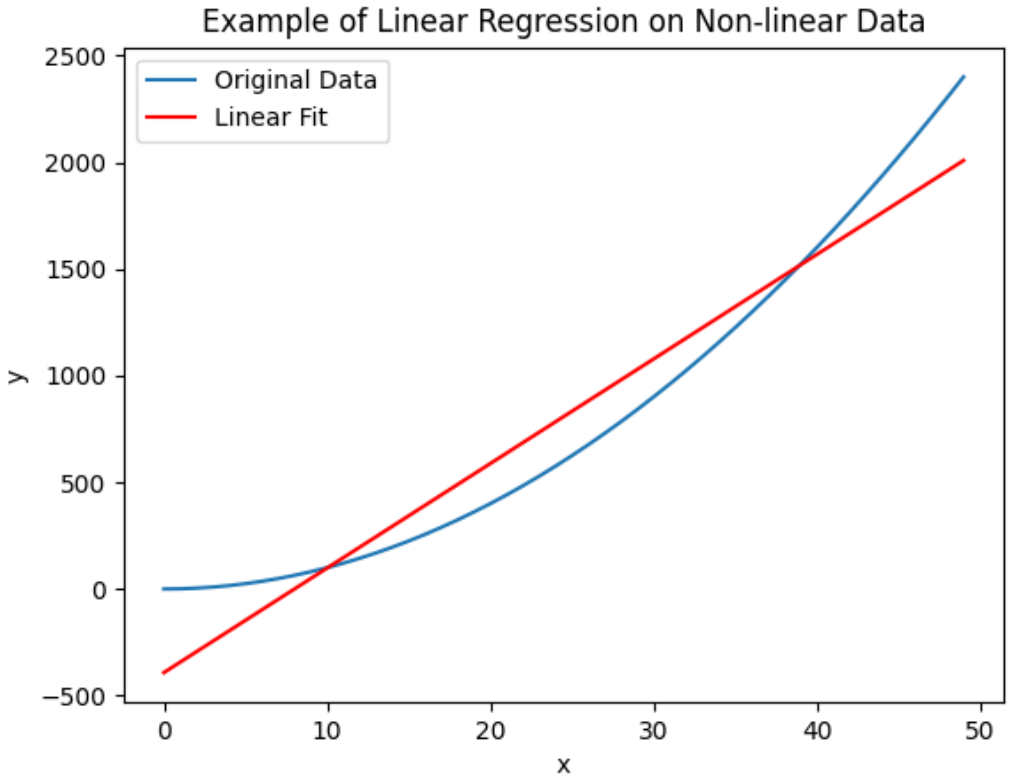

(b) Example of Linear Regression on Non-linear data.

Figure 4.3: Sum offset error for single model.

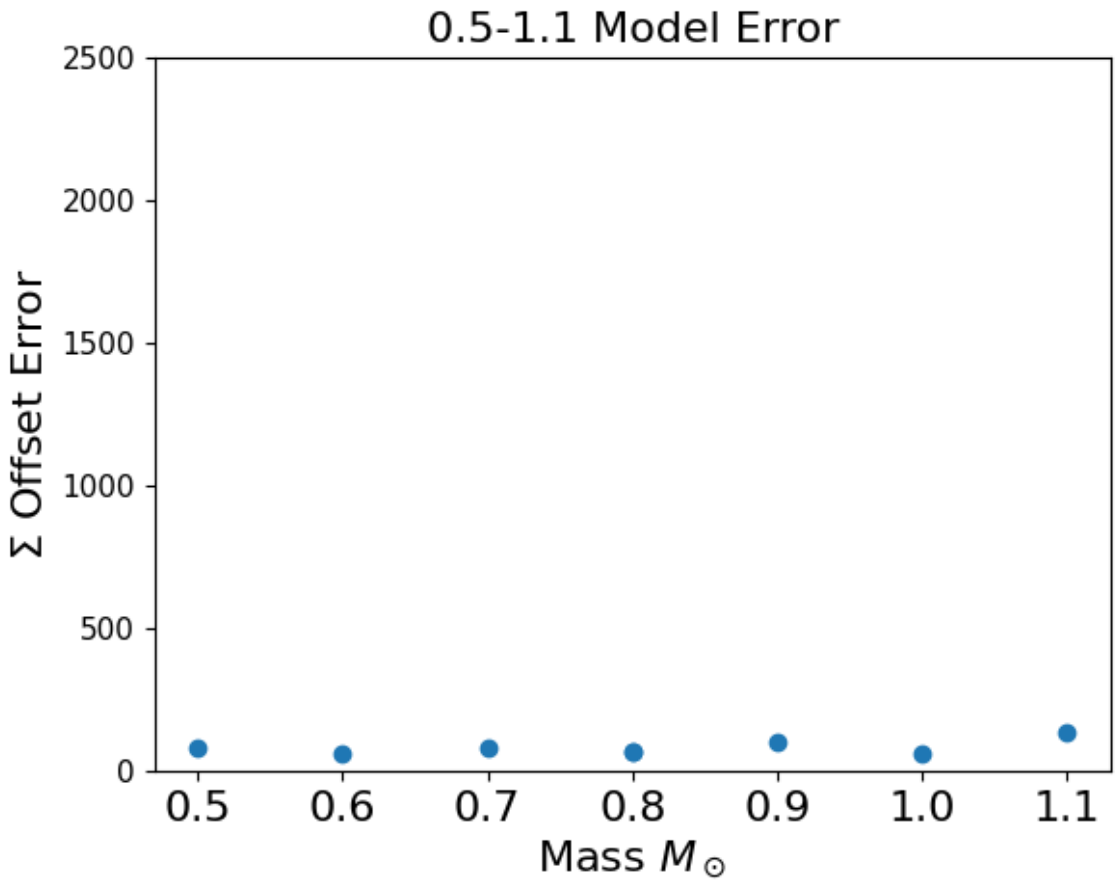

(a) $0.5 - 1.1 M\odot$ Model Error.

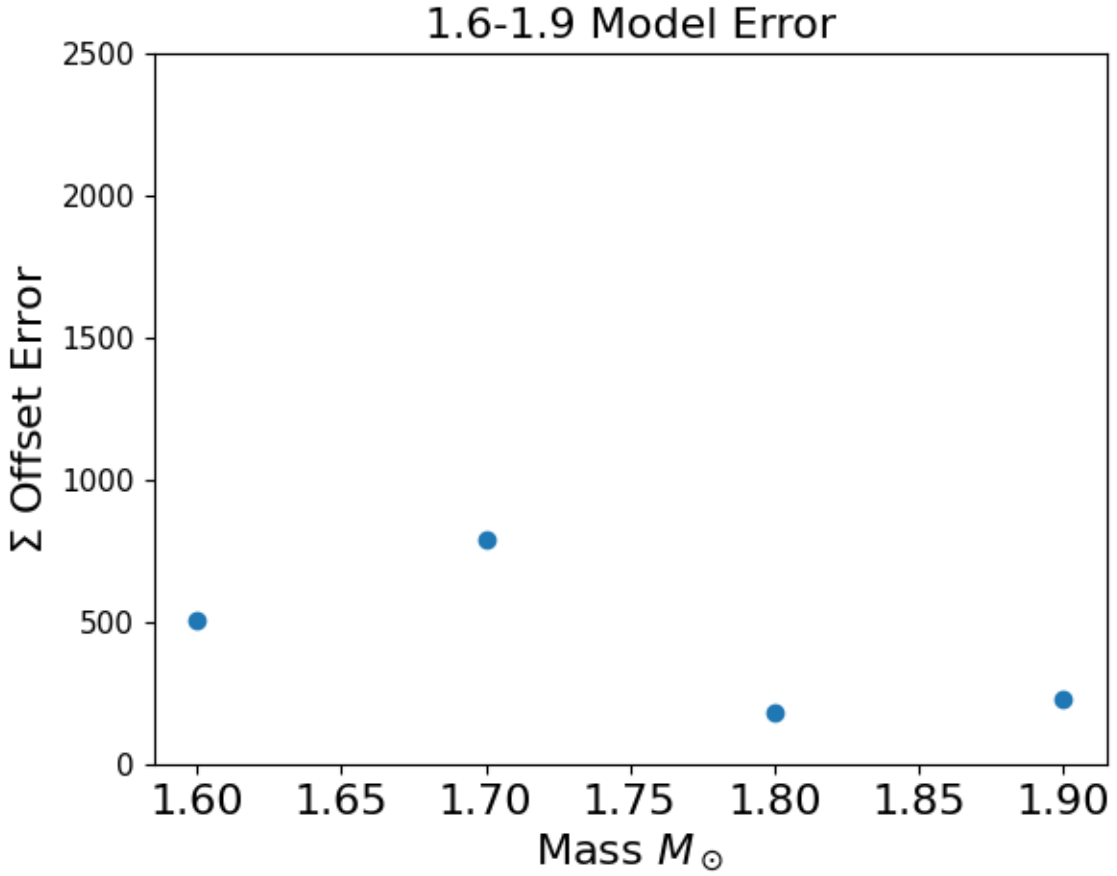

(b) $1.6 - 1.9 M\odot$ Model Error.

Figure 4.4: Sum offset error for multi model.

Figure 4.1 Was both plotted from different model where a is using a single model meaning the linear regression was done using all the data as one model and b is done using multi model meaning that the data is separated into section and linear regression was done on each section separately, for this case the model for $0.5 - 1.1M_{\odot}$. These plots are made by removing $1M_{\odot}$ from the grid to be used as testing data. We can see that for the single model prediction that it is very deviated from the grid and the shape is different from the grid and the multi model prediction strongly follows the $1M_{\odot}$ grid.

The luminosity offset between the 1Mo prediction and 1Mo grid is then calculated and plotted on Figure 4.2. The single model has the smallest offset of around -2.47 and a highest offset of -2.76. The multi model has an upper bound offset of 0.02 and a lower bound of -0.03. From these values we can say that the single model is heavily biased to the negative side and has around 250% error while the multi model has no bias since the offset is balanced and has around 2% error.

This was done across for all the masses for all models as example shown in Figure 4.3a, 4.4a, and 4.4b. However for this plot instead of just calculating the luminosity offset, Formula 3.3 was used in order to calculate the total offset from datapoint to datapoint meaning accounting both luminosity and star age. The show was done using a single model and we can see the error fluctuates quite a lot. This actually indicates that the data is not linear, and after taking a look at the 3D plot Figure A.1, we see that the data have a sort of exponential shape. We can see from the Figure 4.3b as an example where when linear regression is done on a non linear data we can see that the error will be small when the linear fit intercept with the line. However, other than that the error would be huge just like in Figure 4.3a In order to account for this that is why we decided to section the data in order to minimize the error due to the non linearity of the data.

After doing the same analysis on the multi model, we get around the same shape as Figure 4.4a, however when done using the 1.6-1.9 model there is a sudden rise in error. If we look at the data used in this model, we can see that there is large variation especially in the tail section of the plot as seen in Figure A.5. If this variation relates to the real physical variation during stellar evolution we truly cannot use linear regression for this section. The other possibility is that this variation came from artefact, if this is true then we can apply smoothing/outlier removal before doing the linear regression in order to account for this.

4.2 Prediction of Flux

Table 4.1: Stars with their mass and distance.

Star	Mass [$M\odot$]	Distance [pc]
Sun	1	4.85×10^{-6}
τ ceti	0.78	3.65
Sirius	2.06	2.64

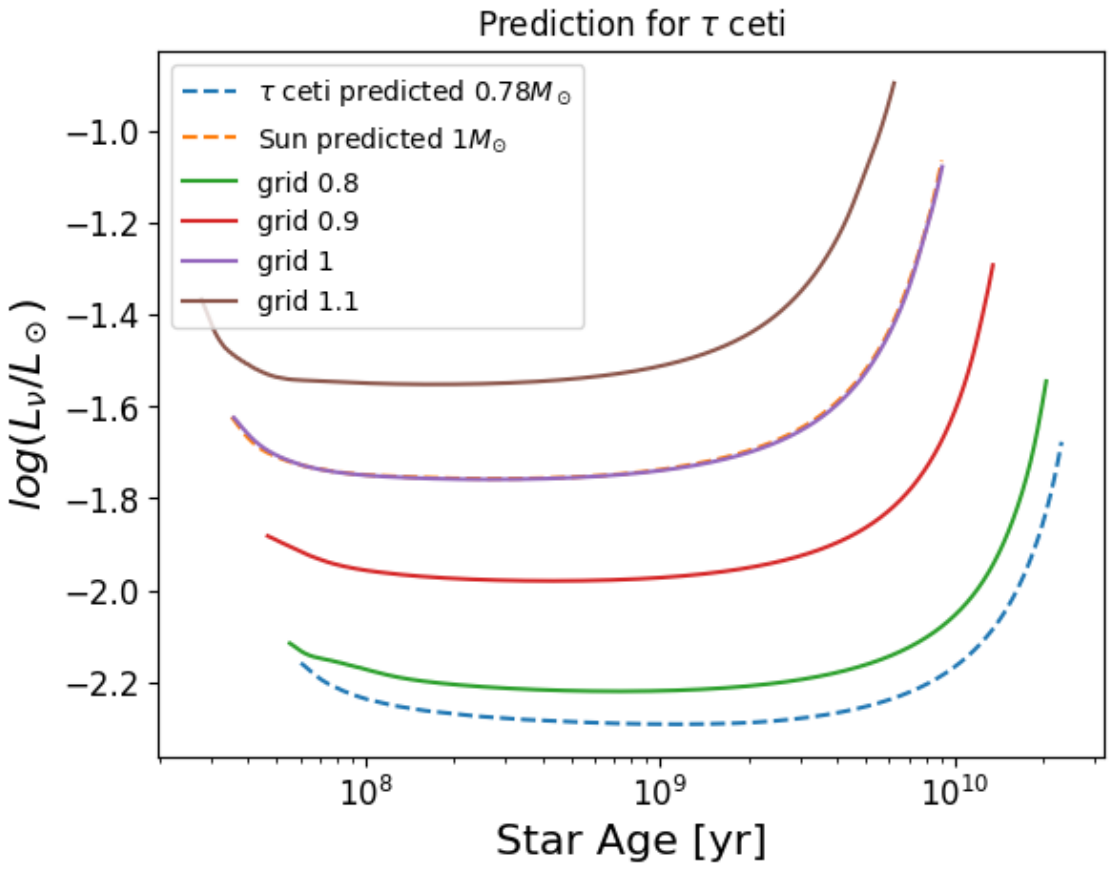

(a) Prediction for τ ceti $0.78M\odot$.

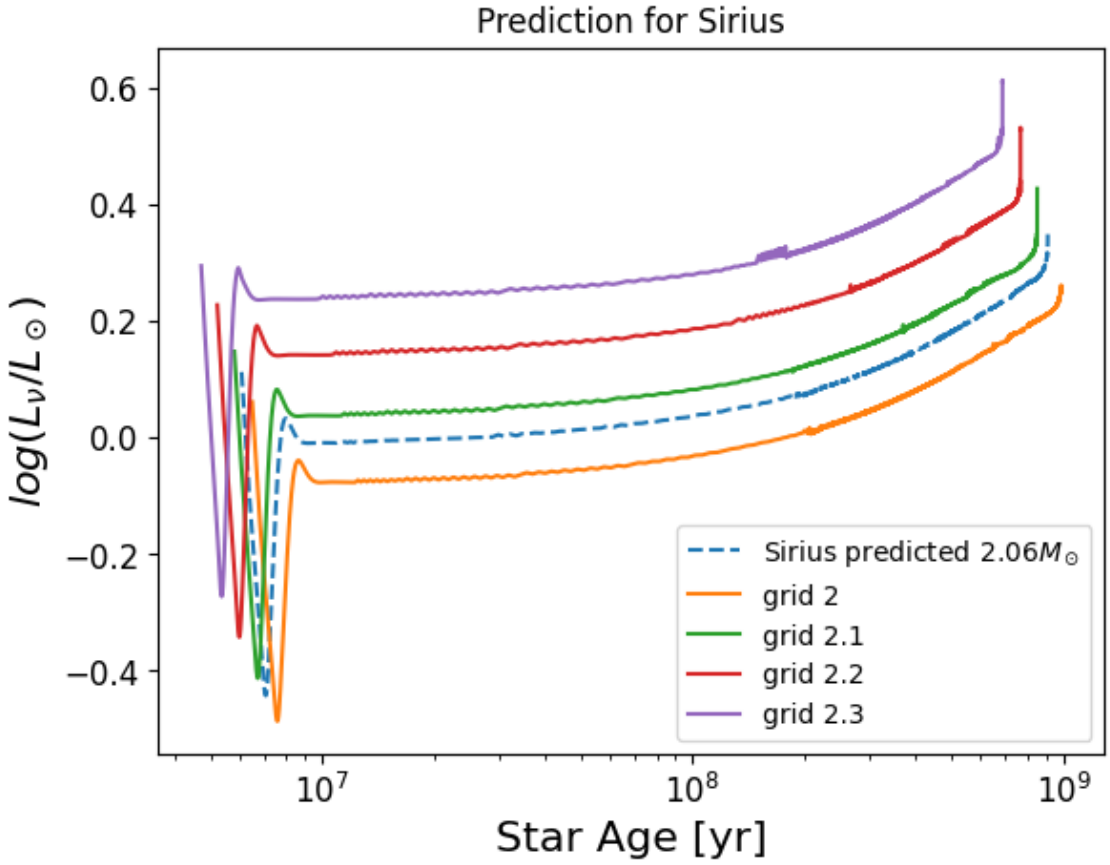

(b) Prediction for Sirius $2.06M\odot$.

Figure 4.5: (
Prediction of different Stars Luminosity and Ages Using Multi Model)

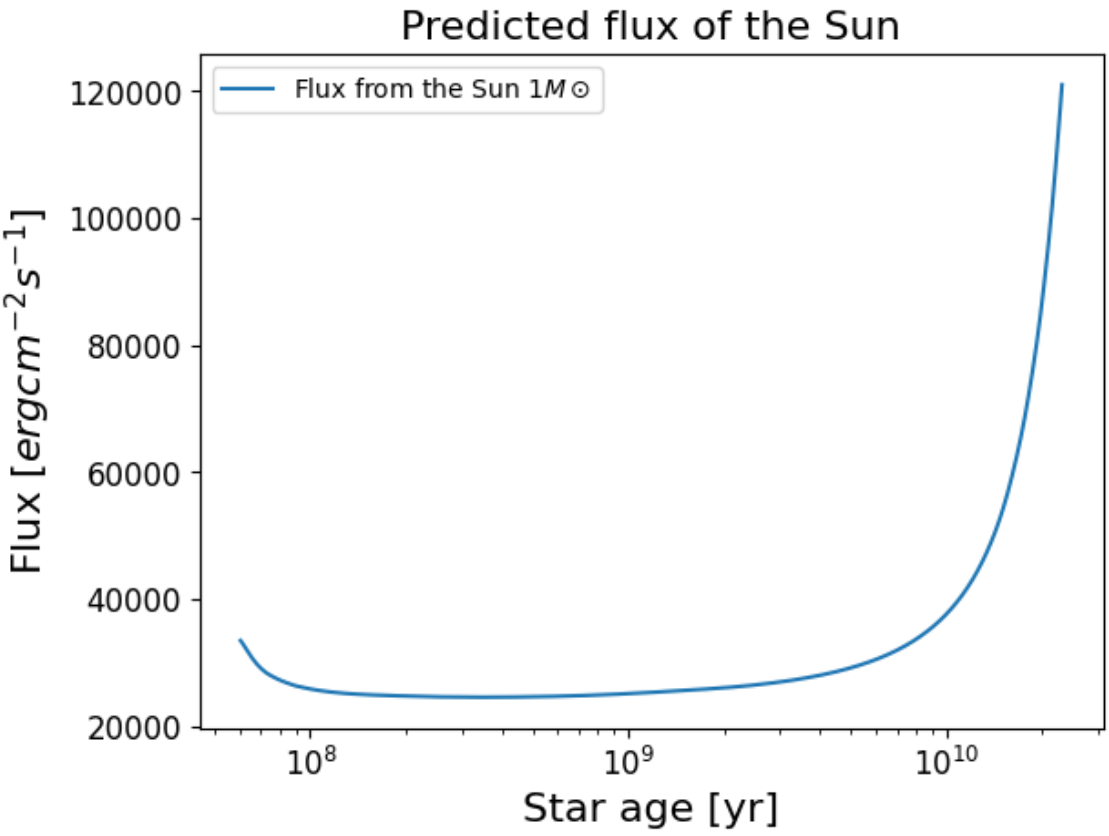

(a) Prediction for Flux of Sun $1M\odot$.

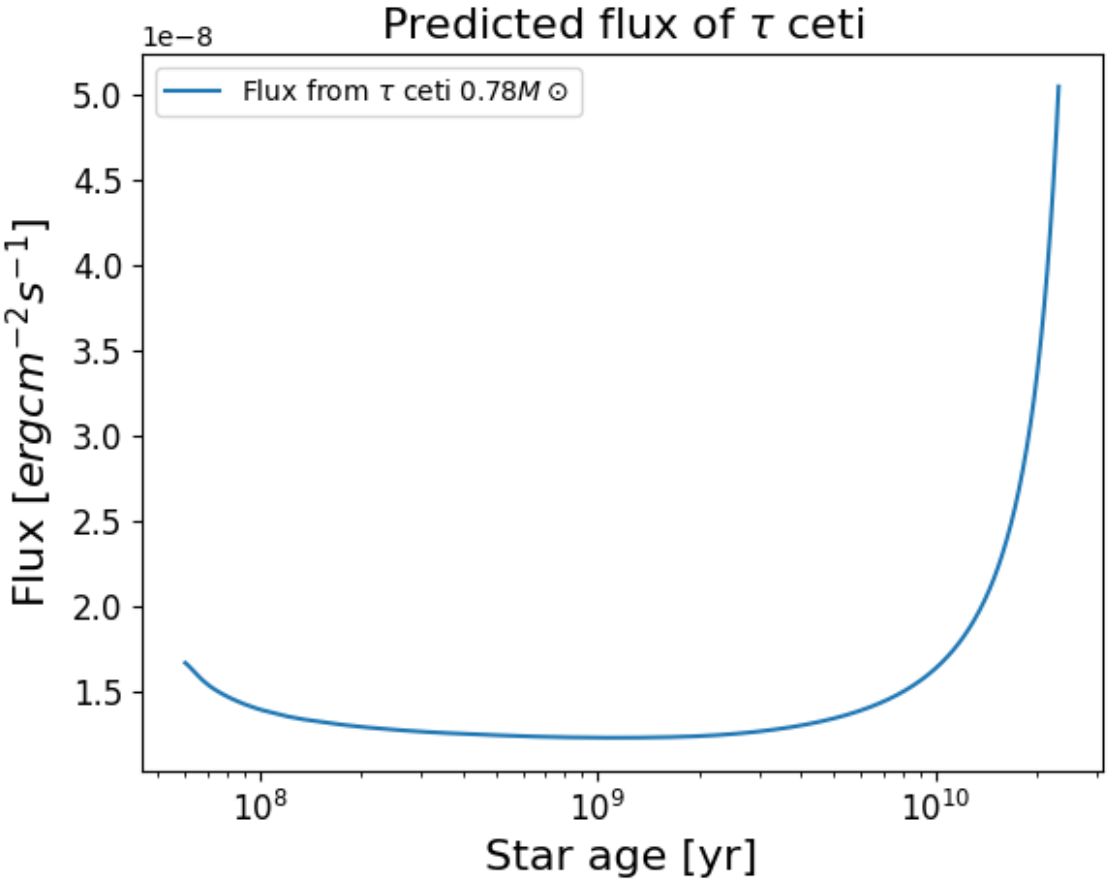

(b) Prediction for flux of τ ceti $0.78M\odot$.

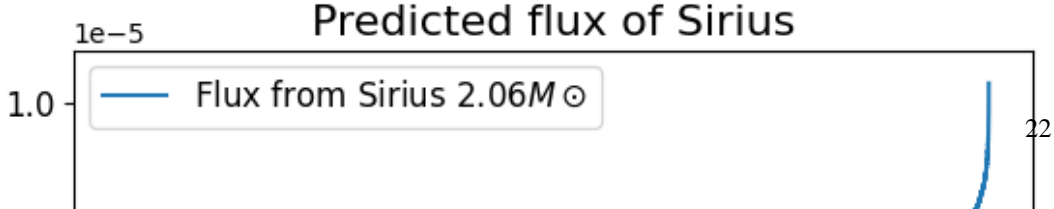

We then decide to use the multi model for prediction of flux from distant stars. We used the data in Table 4.1 to predict flux coming from the Sun and τ ceti where the mass is the mass of the star in term of solar mass and the distance is the distance between the earth and the stars. Figure 4.5a shows plots of $log(l_\nu/l_\odot)$(where $l_\odot = 3.828 \times 10^3 3 ergs^-1$ prediction for t ceti and sun and part of the grid of the model training for comparison. We can see that for the τ ceti with mass $0.78 M_\odot$ it is where we expect it to be, which is below grid 8 and for the sun, it is the same as in Figure 4.1b. The same can be said Sirius with mass of $2.06 M_\odot$ where it is between grid 2 and 2.1. Using the prediction data we then calculate the flux for both the Sun, Sirius and τ ceti as seen in Figure 4.6 The prediction shows that the flux coming from the sun is of 12 orders of magnitude compared to flux coming from tau ceti. When the fluxes are plotted together, the flux of τ ceti will look like it is non-existence. Though Sirius is 2 times more massive than the sun and producing more neutrino, due to the massive different in distance it the neutrino flux on earth are still small by 9 order of magnitude. This is the reason why it is so hard to detect the neutrino coming from these distant stars.

From this we can see that linear regression can be used but it is not the best method. Even after sectioning the data, when met with data that contains huge variation it tends to fail as linear regression is very sensitive to outliers. This means that an even better method needs to be tested, especially one that can handle non-linear data especially in order to incorporate the helium burning stage into the training data in order to predict the neutrino flux coming from that stage of the star's evolution. Methods that can be tested out are neural networks as it is capable of capturing complex patterns in highly non-linear data and may be able to create a more accurate prediction model.

For further testing, cross-validation can be applied to assess model robustness across different data splits, while testing with various data subsets, especially focusing on distinct mass ranges or evolutionary stages, can provide more targeted validation. Incorporating additional astrophysical parameters, such as metallicity or temperature, may capture more variability and improve the model's accuracy. To enhance model performance, strategies like smoothing techniques can reduce noise, and outlier removal can mitigate the impact of anomalous points. Feature engineering can create new, more informative variables, and using model ensembles can balance predictions by leveraging the strengths of multiple models.

CHAPTER 5: CONCLUSION

REFERENCES

Addazi, A., Alvarez-Muniz, J., Alves Batista, R., Amelino-Camelia, G., Antonelli, V., Arzano, M., ... Zornoza, J. (2022). Quantum gravity phenomenology at the dawn of the multi-messenger era—a review. *Progress in Particle and Nuclear Physics*, *125*, 103948. Retrieved from https://www.sciencedirect.com/science/article/pii/S0146641022000096 doi: https://doi.org/10.1016/j.ppnp.2022.103948

Athar, M. S., & Singh, S. K. (2020). *The Physics of Neutrino Interactions*. Cambridge University Press.

Barenboim, G., & Quigg, C. (2003, 4). Neutrino observatories can characterize cosmic sources and neutrino properties. *Physical review. D. Particles, fields, gravitation, and cosmology/Physical review. D. Particles and fields*, *67*(7). Retrieved from https://doi.org/10.1103/physrevd.67.073024 doi: 10.1103/physrevd.67.073024

Bertulani, C. A. (2013). *Nuclei in the cosmos*. World Scientific Publishing Company Incorporated.

Farag, E., Timmes, F. X., Chidester, M. T., Anandagoda, S., & Hartmann, D. (2023a, 11). Stellar neutrino emission across the Mass-Metallicity plane. *Zenodo (CERN European Organization for Nuclear Research)*. Retrieved from https://zenodo.org/record/8327401 doi: 10.5281/zenodo.8327401

Farag, E., Timmes, F. X., Chidester, M. T., Anandagoda, S., & Hartmann, D. H. (2023b, 12). Stellar Neutrino Emission across the Mass–Metallicity Plane. *The Astrophysical Journal Supplement Series*, *270*(1), 5. Retrieved from https://doi.org/10.3847/1538-4365/ad0787 doi: 10.3847/1538-4365/ad0787

Fuller, G. M., & Haxton, W. C. (2022, 1). Neutrinos in stellar astrophysics. *arXiv (Cornell University)*. Retrieved from https://arxiv.org/abs/2208.08050 doi: 10.48550/arxiv.2208.08050

Giunti, C., & Kim, C. W. (2007). *Fundamentals of Neutrino Physics and Astrophysics*. Oxford University Press.

Iliadis, C. (2007). *Nuclear Physics of Stars*. John Wiley & Sons.

Kopp, J., Machado, P., MacMahon, M., & Martinez-Soler, I. (2024). *Improving neutrino energy reconstruction with machine learning*. Retrieved from https://arxiv.org/abs/2405.15867

Krane, K. S. (1991). *Introductory Nuclear Physics*. John Wiley & Sons.

Niu, Z. M., Liang, H. Z., Sun, B. H., Long, W. H., & Niu, Y. F. (2019, 6). Predictions of nuclear β-decay half-lives with machine learning and their impact on r -process nucleosynthesis. *Physical review. C*, *99*(6). Retrieved from https://doi.org/10.1103/physrevc.99.064307 doi: 10.1103/physrevc.99.064307

Overview — Super-Kamiokande Official Webiste. (n.d.). Retrieved from https://www-sk.icrr.u-tokyo.ac.jp/en/sk/about/outline/

Paxton, B., Bildsten, L., Dotter, A., Herwig, F., Lesaffre, P., & Timmes, F. (2010, 12). MODULES FOR EXPERIMENTS IN STELLAR ASTROPHYSICS (MESA). *The Astrophysical Journal Supplement Series*, *192*(1), 3. Retrieved from https://doi.org/10.1088/0067-0049/192/1/3 doi: 10.1088/0067-0049/192/1/3

Rodrigues, F. A. (2023, 10). Machine learning in physics: A short guide. *EPL (Europhysics Letters)*, *144*(2), 22001. Retrieved from https://doi.org/10.1209/0295-5075/ad0575 doi: 10.1209/0295-5075/ad0575

Rosso, A. G., Mascaretti, C., Palladino, A., & Vissani, F. (2018, 7). Introduction to neutrino astronomy*. *The European Physical Journal Plus*, *133*(7). Retrieved from https://doi.org/10.1140/epjp/i2018-12143-6 doi: 10.1140/epjp/i2018-12143-6

Vitagliano, E., Tamborra, I., & Raffelt, G. (2020, 12). Grand unified neutrino spectrum at Earth: Sources and spectral components. *Reviews of Modern Physics*, *92*(4). Retrieved from https://doi.org/10.1103/revmodphys.92.045006 doi: 10.1103/revmodphys.92.045006

Williams, J. H. (2016). *Quantifying measurement*. Morgan & Claypool Publishers.

Zhou, Z.-H. (2021). *Machine learning*. Retrieved from https://doi.org/10.1007/978-981-15-1967-3 doi: 10.1007/978-981-15-1967-3

APPENDIX A: APPENDICES

A.1 Data

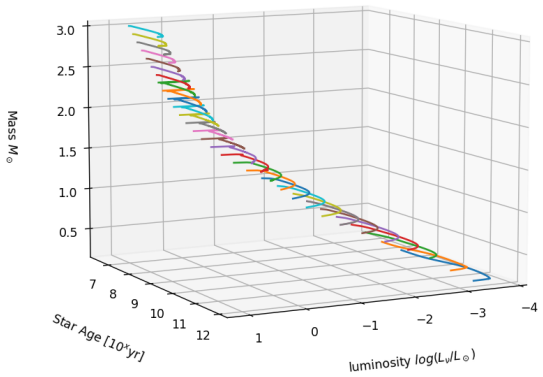

Figure A.1: 3D plot of Data for $0.2 - 3.0 M_\odot$(only H burning).

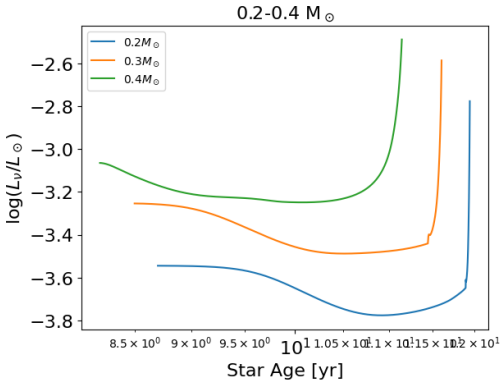

Figure A.2: Data for $0.2 - 0.5 M_\odot$(only H burning).

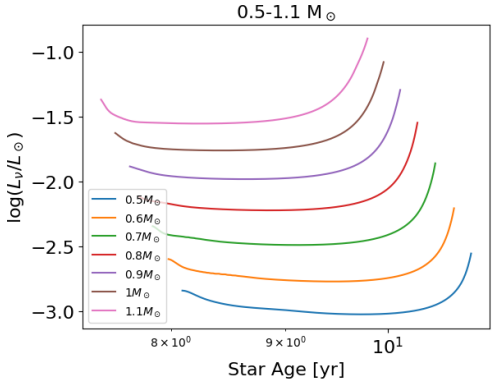

Figure A.3: Data for $0.5 - 1.1 M_\odot$(only H burning).

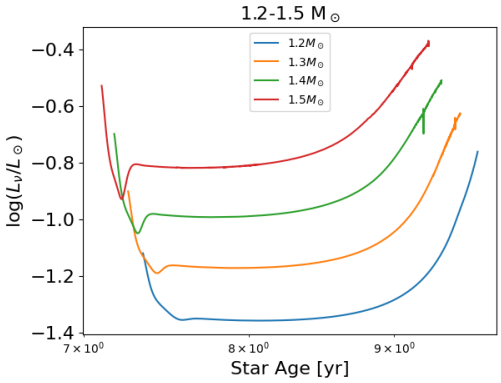

Figure A.4: Data for $1.2 - 1.5 M_{\odot}$(only H burning).

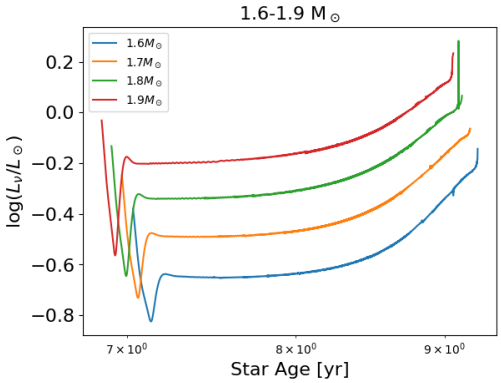

Figure A.5: Data for $1.6 - 1.9 M_{\odot}$(only H burning).

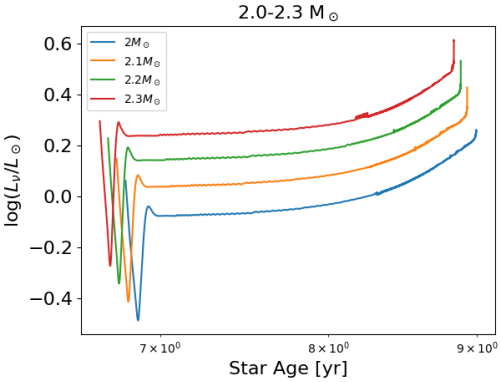

Figure A.6: Data for $2.0 - 2.3 M_{\odot}$(only H burning).

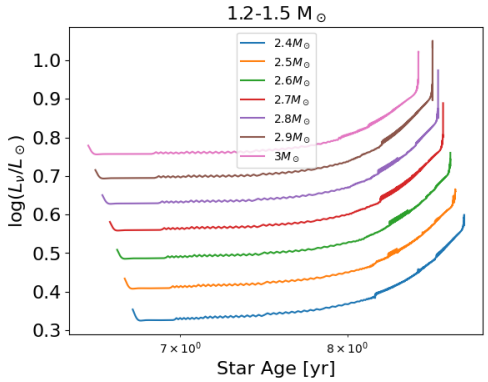

Figure A.7: Data for $2.4 - 3.0 M_{\odot}$(only H burning).